ACOUSTIC NOISE MODELS

by

Henry Cox
New London Laboratory
Naval Underwater Systems Center
New London, Connecticut 06320
USA

ABSTRACT

The question of modeling the vertical directionality of ambient noise in the ocean is considered. The problem of converting from a description in terms of directional density function to a description in terms of the cross-spectral density function between pairs of sensors of arbitrary orientation and separation is examined in detail. Mathematical models which have been used previously are reviewed with special emphasis on spatial harmonic models following closely some material presented earlier. [Cox, J.A.S.A. 54, 1289-1301, (1973)]. The underlying philosophy is that realistic composite models can be obtained by combining a number of simple models each of which models a single significant aspect of the noise field. A new harmonic model is presented for the noise field at the axis of the sound channel due to distant shipping when purely refractive paths dominate. Some simple approximations are developed for the cross-spectral density function in fields dominated by distant shipping.

I Introduction

The spatial correlation of a noise field is a fundamental property in determining the response of an array of sensors. It is therefore desirable to have realistic models of the spatial correlation of ambient noise in the ocean. The ocean, unfortunately, is very complicated and quite variable, making it difficult to model realistically in every detail. Thus, one is forced to compromise.

With the increased availability of large computers, several attempts have been made to develop simulation models in which a number of noise sources is distributed over a geographic area and propagation models are used to compute a sample noise field at the places of interest. With many computer runs using different source distributions, or by allowing the sources to move, estimates of the variability of the noise field can also be obtained. The weaknesses of this type of model lie

in the assumptions about the nature and distribution of noise sources and the weaknesses of whatever propagation model is used. The large computational burden is unattractive for many applications.

The other approach to noise field modeling is the use of mathematical models in which spatial correlation or some equivalent property is described in terms of mathematical functions which can be evaluated by computers with relative ease. The simplest examples of mathematical models are noise which is uncorrelated from sensor to sensor and isotropic noise which results from uncorrelated plane waves of equal intensity propagating in all directions. Even these simple models can lead to difficulties if they are pursued in great detail. The uncorrelated noise model leads to the impractical results that gain of an array against noise can be increased arbitrarily without increasing array aperture by simply increasing the number of sensors. The isotropic noise model leads to the possibility of very high gain, short, superdirective endfire arrays which are impractical because of their extreme sensitivity to amplitude and phase errors in array components. These two simple models also differ in that one is defined directly in terms of the spatial correlation function, that is, uncorrelated noise, while the other, isotropic noise, is defined in terms of a distribution of

uncorrelated plane waves, specifically, a uniform distribution. The difficulties with these models can be reduced by combining them into a simple mixed model. In order to do this we use the information[1] that the cross-spectral density function between two sensors, for instance, the j-th and k-th, separated by a distance s in a spherically isotropic field is $(\sin \omega s/c) / (\omega s/c)$. The simple mixed model then has the following normalized cross-spectral density function: $\alpha \delta_{jk} + (1 - \alpha) (\sin \omega s/c) / (\omega s/c)$.

In this paper, we describe some mathematical models which are a practical middle ground between the cumbersome simulation models and the simple, commonly used, but frequently unrealistic mathematical models described above. While the techniques are broadly applicable, we shall pay particular attention to modeling the vertical directionality of ambient noise in the ocean. The basic approach is to combine different models corresponding to different types of noise sources, in a way similar to mixing of uncorrelated noise and isotropic noise described above.

II Some Basic Definitions

The temporal cross-correlation function between two sensor outputs will be defined as follows

$$q_{12}(\tau) = \overline{n_1(t)\, n_2(t - \tau)} \qquad (1)$$

where the overbar denotes ensemble average. The cross-spectral density function is defined by the following Fourier transformation.

$$Q_{12}(\omega) = \int q_{12}(\tau) \exp(-i\omega\tau)\, d\tau \tag{2}$$

An important example is that of a single plane wave. Let $\underline{p}_1$ and $\underline{p}_2$ be the positions of the two sensors and let $\underline{u}$ be a unit vector in the direction opposite to that in which the plane wave is propagating. Then, if a plane wave propagates past the sensors, the output of the second sensor is a delayed version of the output of the first sensor. That is

$$n_2(t) = n_1[t - \underline{u} \cdot (\underline{p}_1 - \underline{p}_2)/c] \tag{3}$$

where c is the velocity of propagation. Then from Equation (1)

$$q_{12}(\tau) = q_{11}[\tau + \underline{u} \cdot (\underline{p}_1 - \underline{p}_2)/c] \tag{4}$$

and

$$Q'_{12}(\omega) = Q'_{11}(\omega) \exp\left\{i\underline{k} \cdot (\underline{p}_1 - \underline{p}_2)\right\} \tag{5}$$

where

$$\underline{k} = (\omega/c)\underline{u} \tag{6}$$

A spatially homogenous field is one in which the cross-spectral density depends on the relative position $(\underline{p}_1 - \underline{p}_2)$ of two sensors and not on their absolute positions. In such a field $Q'_{12}(\omega)$ is invariant for translations of the sensors but not in general for rotations, and the power spectral density is the same at all points in the field. We shall

be primarily interested in fields which may be considered "locally homogenous", and find it convenient to work with the normalized cross-spectral density

$$Q_{12}(\omega) = Q'_{12}(\omega) / \sqrt{Q'_{11}(\omega)\, Q'_{22}(\omega)} \qquad (7)$$

From Equation (5) it is evident that a single plane wave is an example of a homogenous field. More generally it follows that any superposition of uncorrelated plane waves results in a homogenous field. However, not all homogenous fields may be represented as a superposition of uncorrelated plane waves.

III Distributions of Uncorrelated Plane Waves

1. General

A common approach is to represent a noise field as a sum of uncorrelated plane waves propagating from various directions. Different directional distributions may be used to model different cases. It should be noted that all models of this type can lead to superdirectivity[2] because they are band-limited in spatial frequency[3]. For any directional distribution the noise response of an array can be obtained by multiplying the directional distribution of the noise by the beam pattern of the array and integrating over all directions.

In many problems in modern signal processing it is preferable to describe the noise field in terms of the cross-spectral density between all pairs of elements in the array. Thus, the problem arises

of converting from a representation in terms of directional distributions which are physically intuitive to a representation in terms of cross-spectral densities which are mathematically convenient. This has already been done for the spherically isotropic noise field. For isotropic noise in two dimensions, the normalized cross-spectral density is $J_0(\omega s/c)$ where J_0 is the zeroth-order Bessel function of the first kind. Cron and Sherman[4] modeled the surface of the ocean as a uniform distribution of uncorrelated directional noise sources. With the assumption that the power directivity of the individual sources is $\cos^{2m}(\alpha)$, where α is the angle measured from the downward vertical, they present convenient expressions for the correlation between either horizontally or vertically displaced sensors. Their model is equivalent to a distribution of uncorrelated plane waves which is proportional to $\cos^{2m-1}(\theta)$ for $0 \leq \theta \leq \pi/2$ where θ is measured from the upward vertical. In this model all waves propagate downward, the distribution being zero over the lower hemisphere. For sensors which are displaced from each other in a direction other than vertical or horizontal, this model leads to a complicated integral which describes the spatial correlation. Liggett and Jacobson[5] introduced a single parameter family of directional density functions of the following

form $2A \exp(A \cos \theta) / [\exp(A) - 1]$ for $0 \leq \theta \pi/2$. This leads to a simple expression for the spatial correlation between vertically displaced sensors and a complicated integral for sensors which are aligned other than vertically.

The spatial harmonic approach[3] permits both the directional distribution of uncorrelated plane waves and the orientation of the sensors to be arbitrary. This approach represents the directional density function in terms of spatial harmonics. Each term in the spatial harmonic representation of the directional density leads to a corresponding term in a series of representation of the cross-spectral density between pairs of sensors. Moreover, the coefficients of these corresponding terms are the same and for each term the dependence of the cross-spectral density on the position coordinates of the sensors is factored into components, each of which depends on a single coordinate. The spatial harmonic representation is particularly attractive when the directional density function may be represented by a relatively small number of spatial harmonics so that the series representations involve a correspondingly small number of terms. This is the case for relatively smooth variations in the directional density function. Sharp peaks in this function require many terms in a spatial harmonic model.

For sharply peaked directional noise fields it becomes attractive to model the spatial correlation functions or more precisely the cross-spectral density functions directly. Surprising simple formulae will be presented for such models. Moreover, these simple formulae which are motivated by the results of the spatial harmonic approach, provide good single term approximations to rather involved series arising out of the spatial harmonic approach.

2. Azimuthally Uniform Fields

In order to study the vertical directionality of ambient noise, it is convenient to make the simplifying assumption that the field is azimuthally uniform and that only angles measured from the vertical are relevant. This assumption is adequate for dealing with data from vertical line arrays since such arrays have azimuthal symmetry and cannot sense azimuthal variations in a noise field.

Consider an azimuthally uniform field in which the density of uncorrelated plane waves is $F(\theta, \omega)$ when θ is measured from the vertical. For convenience, we normalize so that

$$\frac{1}{2} \int_0^{\pi} F(\theta, \omega) \sin\theta \, d\theta = 1 \tag{8}$$

For two sensors which are separated by a distance s along a line which makes an angle γ with the vertical, the normalized cross-spectral density

may be expressed as

$$Q(s, \omega; \gamma, \zeta) = (1/2) \int_0^{\pi} J_0[(\omega s/c) \sin\gamma \ \sin\theta] \ F(\theta, \omega) \exp\left\{ i(\omega s/c) \cos\gamma \ \cos\theta \right\} \sin\theta \ d\theta \tag{9}$$

The notation $Q(s, \omega; \gamma, \zeta)$ signifies the cross-spectral density function between two sensors separated by a distance s along a line which has a vertical angle γ and an azimuthal angle ζ. For azimuthally uniform fields the expression is independent of ζ.

Equation (9) is the basic relationship between the cross-spectral density functions and the directional density function for fields consisting of azimuthally uniform distributions of plane waves. It simplifies for $\gamma = 0$, vertically displaced sensors, the Bessel function being unity, and for horizontally displaced sensors $\gamma = \pi/2$, where the exponential is unity. The strategy in modeling noise fields of this type is basically to choose a directional distribution such that the integral in Equation (9) simplifies.

An elementary example in which this integral simplifies is one in which all the noise comes from two vertical angles of arrival which are symmetric about the horizontal. This model arises in the study of the deep sound channel. Let

$$F(\theta, \omega) \sin\theta = \delta(\theta - \theta_0) + \delta(\theta - \pi + \theta_0) \tag{10}$$

where δ is the Dirac delta function. Then

$$Q(s, \omega ; \gamma, \zeta) = J_0 [(\omega s/c) \sin\gamma \sin \theta_0] \cos [(\omega s/c) \cos\gamma \cos \theta_0] \qquad (11)$$

For the case $\theta_0 = \pi/2$ and $\gamma = \pi/2$ Equation (1) reduces to the classical result for a cyclindrically isotropic field. Figure 1 displays the classical results for isotropic fields. Figure 2, presents plots of Equation (11) for the case $\theta_0 = 72^o$ and various values of γ. Notice the transition from the simple cosine function for $\gamma = 0$ to the zeroth order Bessel function for the case $\gamma = 90^o$.

In the model of Cron and Sherman

$$F(\theta, \omega) = \begin{cases} 4m \cos^{2m-1}(\theta), & 0 \le \theta \le \pi/2 \\ 0, & \pi/2 < \theta \le \pi \end{cases} \qquad (12)$$

where m is a parameter. When this expression is substituted into Equation (9), the following result is obtained for horizontally separated sensors

$$Q(s,\omega; \pi/2, \zeta) = 2^m m!\, J_m(\omega s/c) / (\omega s/c)^m \qquad (13)$$

For vertically separated sensors, the same substitution leads to

$$Q(s,\omega; 0, \zeta) = 2m \int_0^1 x^{2m-1} \exp \{ i(\omega s/c) x \} \, dx \qquad (14)$$

where $x = \cos\theta$. For any value of m, Equation (14) may be integrated by parts.

Liggett and Jacobson introduced the following family of models which depend on a parameter A:

$$F(\theta,\omega) = \begin{cases} 2A\ \exp(A\cos\theta) \,/\, [\exp(A) - 1], & 0 \le \theta \le \pi/2 \\ 0, & \pi/2 < \theta \le \pi \end{cases} \tag{15}$$

This model has the advantage of not requiring the maximum of $F(0,\omega)$ to occur at $\theta = 0$, as did the $4m \cos^{2m-1}(\theta)$ model. Substituting from Equation (15) into Equation (9), leads to the following simple result for vertically separated sensors:

$$Q(s,\omega;\, 0,\zeta) = \left[\frac{A}{\exp(A) - 1}\right]\left[\frac{\exp\{i(\omega s/c) + A\} - 1}{i(\omega s/c) + A}\right] \tag{16}$$

Another approach is to represent the directional density in terms of spatial harmonics. This general approach applying to both two-dimensional and three-dimensional fields has been discussed in detail previously[3]. For the case of azimuthally uniform fields, $F(\theta, \omega)$ is described in terms of the so-called zonal harmonics as follows

$$F(\theta,\omega) = \sum_{n=0}^{\infty} c_n(\omega)\, P_n(\cos\theta), \qquad 0 \le \theta \le \pi \tag{17}$$

where $P_n(\cos\theta)$ is a Legendre polynomial of the first kind. Substituting from Equation (17) into Equation (9) and integrating yields the following series representation for the cross-spectral density function

$$Q(s, \omega; \gamma, \zeta) = \sum_{n=o}^{\infty} i^n c_n(\omega) P_n(\cos\gamma) j_n(\omega s/c) \tag{18}$$

when j_n is the n-th order spherical Bessel function of the first kind. Notice that the coefficients c_n are identical in Equations (17) and (18) and that the dependence on the orientation γ and the separation s of the sensors is factored in each term in Equation (18).

As was mentioned earlier the spatial harmonic representation is most attractive when the field of interest can be represented adequately by a series which has only a few non-zero terms. This is the case for relatively smooth angular variations in the directional density function. Sharp variations require many terms. The models of Cron and Sherman and Liggett and Jacobson which are zero over the lower hemisphere require an infinite number of spatial harmonics. The model of Equation (10) which involves the Dirac delta function also requires an infinite series.

IV Ocean Noise Models

In a paper[6] which has become a classic, Wenz discussed the frequency dependence of the level of ambient noise measured by omni-directional

sensors and related the noise in different frequency regions to different sources. For frequencies above about 500 Hertz, there is a strong dependence of the ocean ambient noise level on wind speed, and the noise is usually attributed to surface waves. In the frequency region 20 to 100 Hertz, little dependence on wind speed has been reported and noise is attributed to shipping. A cross-over usually occurs in the region 100 to 500 Hertz, where shipping noise and surface wave noise both contribute. The frequency of this cross-over from shipping noise to surface wave noise depends on shipping density and wind speed.

Perrone[7] presented an in depth study of the dependence of ambient noise level on wind speed for a site off Bermuda during the month of January. His data show a clear wind speed dependence above 112 Hertz and also some evidence of a wind speed dependence below 17 Hertz.

When considering shipping noise it is useful to distinguish between that due to a few nearby ships and that caused by a large number of ships at great ranges. Noise due to distant shipping is expected to be less variable than that due to local traffic since it results from a large number of contributing ships. Distant shipping noise arrives from angles near the horizontal since rays at steep angles are

attenuated severely by multiple interactions with the ocean bottom. Its detailed vertical structure can be expected to depend on depth. For example, near the critical depth all purely refracted rays which begin at the surface are concentrated in a small angular region about the horizontal. Near the axis of the sound channel, purely refracted rays which originate at the surface are concentrated into upward and downward going bundles in the region of from about 10 to 20 degrees from the horizontal with no purely horizontal components. Of course, variation of the sound velocity structure with range, and reflection of sound by sea mounts and the sides of ocean basins modify this simple picture. Local traffic noise tends to arrive from discrete angles in azimuth and elevation as indicated by the ray paths from the individual sources to the point of interest.

Surface wave noise tends to be local in origin and to arrive more from the overhead than the horizontal.

Our approach to ocean noise modeling will be to develop models for each of the principal components and to combine these components as appropriate to model the situation of interest.

We begin by considering distant shipping noise. Figure 3 presents curves of directional density of ambient noise at 112 Hertz reported by Axelrod, Schoomer and Von Winkle[8] for Beaufort wind force 4 and 5

based on measurements with a deep, bottom moored vertical line array near Bermuda. They did not report on directions below the horizontal. Also shown in Figure 3 are the curves 10 log$[A_8(\theta)]$ and 10 log $[A_{20}(\theta)]$ where

$$A_8(\theta) = (1/60) + (59/60)\sin^8\theta \tag{19}$$

and

$$A_{20}(\theta) = a + (1 - a)\sin^{20}\theta \tag{20}$$

for a = .001, .003 and .01. For ease of comparison in the figure these curves are normalized to have unit values at their maxima. Hence $A_8(\theta)$ and $A_{20}(\theta)$ have to be renormalized to satisfy Equation (8) which is a power normalization.

Functions of the form $\sin^{2m}\theta$ are attractive for modeling low frequency noise because of their peak horizontal ($\theta = \pi/2$) and because they have no side lobes. They may be represented by a finite series of m + 1 Legendre polynomials as follows

$$\sin^{2m}\theta = \sum_{n=o}^{m} a_{2n} P_{2n}(\cos\theta) \tag{21}$$

Table I lists the coefficients a_{2n} of the Legendre polynomial expansion of $\sin^8(\theta)$ and $\sin^{20}(\theta)$.

Notice that the $\sin^{20}$ model with eleven terms in its series representation is more sharply directional than the $\sin^{8}$ model which has only five terms in its series representation. A small isotropic component is included in Equations (19) and (20) to better fit the data near $\theta = 0$. Eleven term models which are somewhat more directional than $\sin^{20}(\theta)$ can be developed but they will have sidelobes. The sidelobes and nulls can be covered by adding an isotropic component. The problem of designing series with a few terms which compromise between mainlobe shape and sidelobe level is analogous to designing digital filters or shading for arrays. However, highly directional fields require more terms in their series.

The scaling required to satisfy Equation (8) is simply that required to make the coefficient of P_0 equal to unity, because the Legendre polynomials are orthogonal. Let $F_{20}(\theta) = b\, A_{20}(\theta)$ be the appropriately normalized version satisfying Equation (8), then by substituting from Equations (20) and (21) into Equation (18) we obtain

$$Q(s, \omega ; \gamma, \zeta) = ab + (1 - a)\, b \sum_{n=0}^{10} (-1)^n a_{2n} P_{2n}(\cos \gamma)\, j_{2n}(\omega s/c) \qquad (22)$$

Notice that the odd terms in Equation (18) drop out so that the cross-spectral density is purely real. This is due to the fact that the directional density function is symmetric about the horizontal so that there is no net flow of power in any direction.

Figure 4 presents plots of cross-spectral density functions computed from Equation (22) for $\gamma = 0$, 30, 60 and 90 degrees and similar plots for $F_8(\theta)$. The effect of narrowing the width of the noise lobe at $\theta = \pi/2$ by going from $F_8(\theta)$ to $F_{20}(\theta)$ is most evident for vertically separated sensors ($\gamma = 0$) where a significant increase in correlation occurs. The effect on horizontal sensors is very small. In the limit of all the noise coming from the horizontal, the cross-spectral density would become unity for vertically separated sensors and $J_0(2\pi s/\lambda)$ for horizontally separated sensors. Thus, the decrease in coherence with increased separation of vertical sensors is due to the finite width of the noise lobe. A comparison of Figures 1 and 4 shows that the cross-spectral density for horizontally separated sensors when $F(\theta) = F_8(\theta)$ or $F_{20}(\theta)$ is already quite similar to the limit $J_0(2\pi s/\lambda)$. Moreover the curves for $\gamma = 60$ degrees look very much like damped versions of $J_0[(2\pi s/\lambda)\sin\gamma)]$ which is what we would expect from setting $\theta_0 = \pi$ in Equation (11).

It is indeed tempting to try to approximate the curves of Figure 4 by a damped Bessel function. From the shape of the curves for $\gamma = 0$, a Gaussian damping looks attractive. We expect the correlation length, or the width of the Gaussian function to be inversely proportional to the width of the noise lobe. Let $\Delta\theta$ be the half width of the noise lobe

to the 3 dB point. Then we may define a correlation length L by

$$\sin \Delta\ \theta = \lambda / (2L \cos \gamma) \tag{23}$$

An appropriate constant is needed to relate to the correlation length to the quantity which plays the role of "standard deviation" in the Gaussian function. The constant 3/8 seems to work reasonably well. Thus we are led to the following expression for Gaussian damping

$$D(\Delta\theta) = \exp\left\{-\frac{1}{2}(8s/3L)^2\right\} \tag{24}$$

or combining Equations (23) and (24)

$$D(\Delta\theta) = \exp\left\{-14.2\left[(s \sin \Delta\theta \cos \gamma)/\lambda\right]^2\right\} \tag{25}$$

Thus, we are led to approximate the curves of Figure 4 by the following

$$Q_{90}(s,\omega;\gamma,\zeta,\Delta\theta) = D(\Delta\theta)\, J_0[(2\pi s/\lambda)\sin\gamma] \tag{26}$$

where the subscript 90 reminds us that the noise lobe is at the horizontal, 90 degrees. From Figure 3 it is found the $\Delta\theta$ is equal to about 15 degrees for the $\sin^{20}$ model and 23.5 degrees for the $\sin^{8}$ model. Using these values we find that Equation (26) is a good approximation to the curves of Figure 4, especially for the $\sin^{20}$ case. It is therefore a good single term approximation to the eleven term series of

Equation (22). Equation (26) is a correlation model since it describes the cross-spectral density functions directly. It is particularly attractive for sharp noise lobes such as one would expect to find at the critical depth at frequencies where distant shipping is the dominant source of noise.

Arase and Arase[9] reported measurements of normalized spatial correlation at zero time delay of low frequency noise. Sensors were bottom mounted and filters of finite bandwidth were used. Their data are shown in Figure 5 along with the corresponding curve for the $\sin^{20}$ model, corrected for bandwidth. The agreement is good but not much should be concluded since such a wide range of models give approximately the same result $J_0(2\pi s/\lambda)$ for horizontally separated sensors.

In order to model noise at the axis of the sound channel due to distant shipping when purely refractive paths dominate, we would like a model which has a notch at the horizontal. A spatial harmonic model with this characteristic can be obtained by multiplying $\sin^{20}(\theta)$ by $\cos^2(\theta)$. Using the relationship

$$\cos^2(\theta)\sin^{20}\theta = \sin^{20}\theta - \sin^{22}\theta \qquad (27)$$

we see that this case may be treated using the basic $\sin^{2n}$ model by differencing. The directional density $F_{20} - F_{22}$ is shown in Figure

6 and the corresponding cross-spectral density curves are shown in Figure 7. It should be mentioned that the subtraction process involved in this model is very sensitive, requiring high precision in computation. It is analogous in a way to superdirectivity. A comparison of Figures 2 and 7, lead us to try to model this situation by a damped version of Equation (11). For the case of interest in which θ_o is near the horizontal, such an approximation is

$$Q_d(s, \omega; \gamma, \zeta, \Delta\theta, \theta_o) = D(\Delta\theta)\, J_o[(\omega s/c) \sin\gamma \sin\theta_o] \cdot \cos[(\omega s/c) \cos\gamma \cos\theta_o] \quad (28)$$

where the subscript d reminds us of the double peaked nature of the noise field. Using $\Delta\theta$ of 10 degrees from Figure 6 and θ_o of 72 degrees in Equation (28) gives a reasonable approximation to the curves of Figure 6. Thus, Equation (28) is a useful correlation model of sound channel axis noise due to distant shipping. Using $\theta_o = 83.5^o$ and $\Delta\theta = 7.5^o$, Equation (28) may also be used to model the $\sin^{20}$ field.

Turning our attention to the surface wave noise which is characteristic of frequencies above 500 Hertz, we shall follow closely the treatment of the earlier paper[3]. Axelrod, Schoomer and Von Winkle present curves of directional density at 891, 1122 and 1414 Hertz for a number of wind speed conditions. The shape of their curves is quite insensitive to wind speed in this frequency range. An

example of their results, that at 1122 Hertz and Beaufort wind force 5, is given in Figure 8. Also shown in the figure are the Cron and Sherman model $F(\theta) \sim \cos\theta$, for $0 \leq \theta \leq \pi/2$ and a simple four term harmonic model

$$A_h(\theta) = .1 + .9[\sin(2\theta) / 4\sin(\theta/2)]^2 \tag{29}$$

where the subscript h reminds us that it is a high frequency model. This simple model is seen to be in good agreement with the results of Axelrod, Schoomer and Von Winkle for the region $0 \leq \theta \leq \pi/2$ which they report. The model gives about 10 dB more noise from $\theta = 0$ than from $\theta = \pi/2$ and $\theta = \pi$.

Since the function $[\sin(2\theta) / 4\sin(\theta/2)]^2$ may be expressed as a cosine series it is a simple matter to represent it in terms of Legendre polynomials as follows

$$[\sin(2\theta) / 4\sin(\theta/2)]^2 = (1/6) + (3/10) P_1(\cos\theta) + (1/3) P_2(\cos\theta) + (1/5) P_3(\cos\theta) \tag{30}$$

Figure 9 presents graphs of the real and imaginary parts of $Q(s, \omega; \lambda, \zeta)$ when the field is described by $F_h(\theta)$ which is a normalized version of $A_h(\theta)$. The imaginary part results from the net flow of noise power downward due to the asymmetry of $F_h(\theta)$ about $\theta = \pi/2$. The imaginary part for $F_h(\theta)$ does not have as high a peak

value as it would for the Cron and Sherman model since the asymmetry of the $F_h(\theta)$ model is not as great as that of their model in which $F(\theta)$ is zero for $\pi/2 \leq \theta \leq \pi$.

Figures 10 and 11 compare zero time-delay spatial correlations of vertically separated sensors reported by Cron, Hassell and Keltonic[10] with those computed using the $F_h(\theta)$ model. The agreement is quite good.

So far, we have presented a number of mathematical models for distant shipping noise and surface wave noise. These models all give closed form expressions for the cross-spectral density functions. However, the underlying philosophy is that a noise field should be modeled by a composite of models each of which models an important feature of the noise field. It is particularly easy to combine models which are expressed in terms of the cross-spectral density function. Indeed, in the usual case of uncorrelated noise sources the cross-spectral density functions may be combined linearly.

For example, if an intermediate frequency noise model is formed using a linear combination of $F_h(\theta)$ and $F_{20}(\theta)$, the cross-spectral density function is easily obtained from those already computed for these components of the model.

Figure 12 illustrates linear combinations of $F_{20}(\theta)$ with a = .001 and $F_h(\theta)$ of form

$$F(\theta) = B\ F_h(\theta) + (1-B)\ F_{20}(\theta) \tag{31}$$

where the values B = .01, .1, .5 and .8 are shown. Figure 13 presents zero time-delay spatial correlations at 250 Hertz reported by Arase and Arase for vertically separated hydrophones in a sea state 5. Also shown is the curve based on the model of Equation (32) with B = .8 so that there is 6 dB more surface noise than shipping noise. Again the agreement is quite good. Average ambient noise level curves such as those given by Urick[11] indicate that for sea state 5 at 250 Hertz, 6 dB more surface noise than shipping noise would be consistent with a moderate shipping density. Thus the value B = .8 is intuitively reasonable.

Conclusion

The models described in this paper may be combined with other models such as a plane wave from (θ, ϕ) for which

$$Q(s, \omega; \gamma, \zeta) = \exp\left\{ i(\omega s/c)\ [\sin\theta\ \sin\gamma\ \cos(\phi - \zeta) + \cos\theta\ \cos\gamma\ ] \right\} \tag{32}$$

which can be used to model nearby discrete sources, independent noise which models electronic noise and phase imbalance between sensors, and an exponentially decreasing magnitude of cross-spectral density which models flow noise.

By using an appropriate composite, it is possible to obtain computationally attractive, physically motivated, mathematical models which are in agreement with reported data and are far more realistic than the simplistic models which are so commonly employed in the field of sonar.

REFERENCES

1. C. Eckart, J. Acoust. Soc. Am. 25, 195-203, (1953).
2. T. Kooij and H. Cox, "Superdirectivity Revisited" presented at 90th meeting of The Acoustical Society of America, San Francisco, Nov. 1975.
3. H. Cox, J. Acoust. Soc. Am. 54, 1289-1301 (1973).
4. B. F. Cron and C. H. Sherman, J. Acoust. Soc. Am. 34, 1732-1736 (1962).
5. W. S. Liggett, Jr., and M. J. Jacobson, J. Acoust. Soc. Am. 39, 280-288 (1966).
6. G. Wenz, J. Acoust. Soc. Am. 34, 1936-1956 (1962).
7. A. J. Perrone, J. Acoust. Soc. Am. 46, 762-770 (1969).
8. E. H. Axelrod, B. A. Schoomer, and W. A. Von Winkle, J. Acoust. Soc. Am. 37, 77-83 (1965).
9. E. M. Arase and T. Arase, J. Acoust. Soc. Am. 40, 205-210 (1966).
10. B. F. Cron, B. C. Hassell, and F. J. Keltonic, J. Acoust. Soc. Am. 37, 523-529 (1965).
11. R. J. Urick, Principles of Underwater Sound for Engineers, (McGraw-Hill, New York, 1967) p 168.

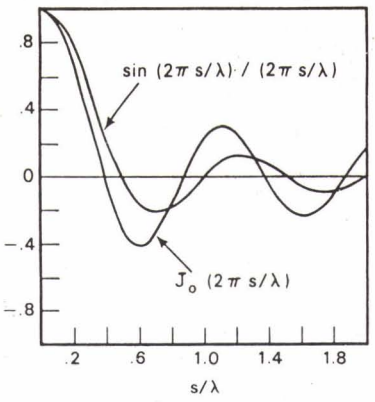

FIG. 1
CROSS-SPECTRAL DENSITY FUNCTIONS FOR ISOTROPIC FIELDS (From Ref. 3)

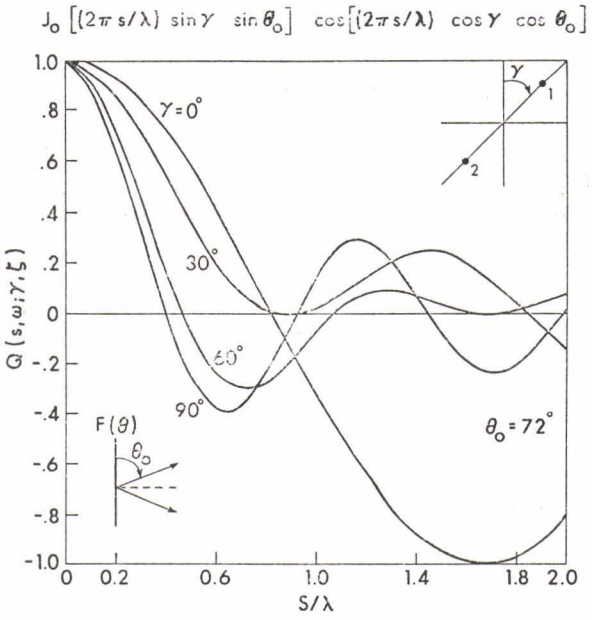

FIG. 2
CROSS-SPECTRAL DENSITY FUNCTIONS FOR A FIELD OF TWO SYMMETRIC DISCRETE ARRIVALS

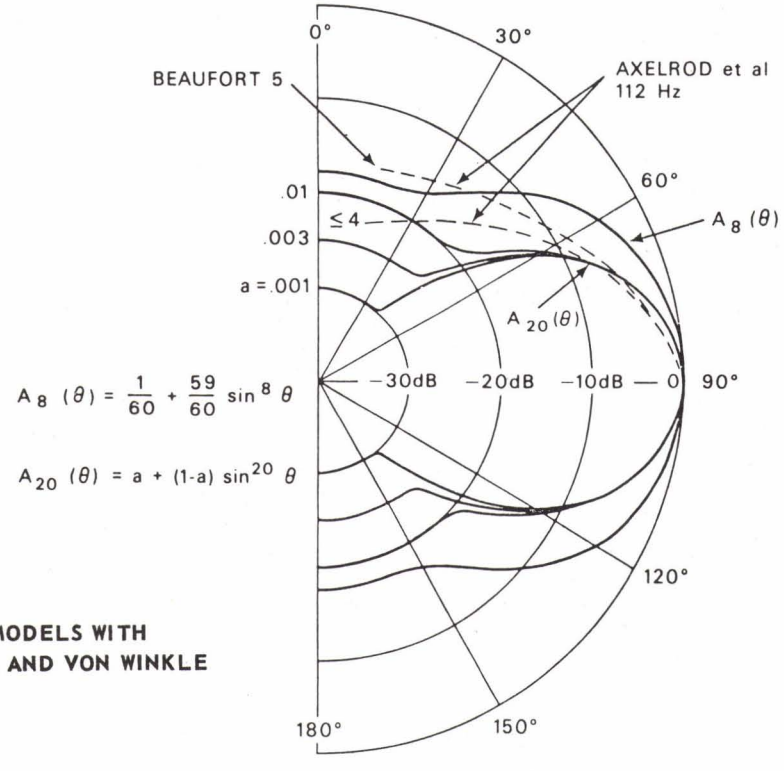

FIG. 3
COMPARISON OF LOW FREQUENCY NOISE MODELS WITH MEASUREMENTS OF AXELROD, SCHOOMER AND VON WINKLE (From Ref. 3)

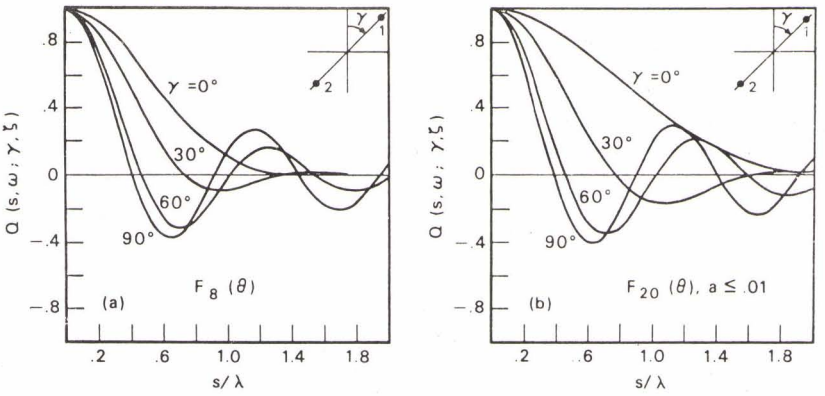

FIG. 4 CROSS-SPECTRAL DENSITY FUNCTIONS FOR VARIOUS SENSOR ORIENTATIONS AND SPACINGS COMPUTED FOR $F_8(\theta)$ AND $F_{20}(\theta)$ MODELS (From Ref. 3)

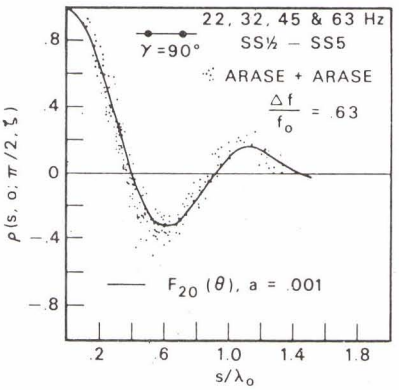

FIG. 5
COMPARISON OF NORMALIZED ZERO TIME-DELAY SPATIAL CORRELATION MEASUREMENTS OF ARASE AND ARASE WITH THAT DERIVED FROM THE $F_{20}(\theta)$ MODEL (From Ref. 3)

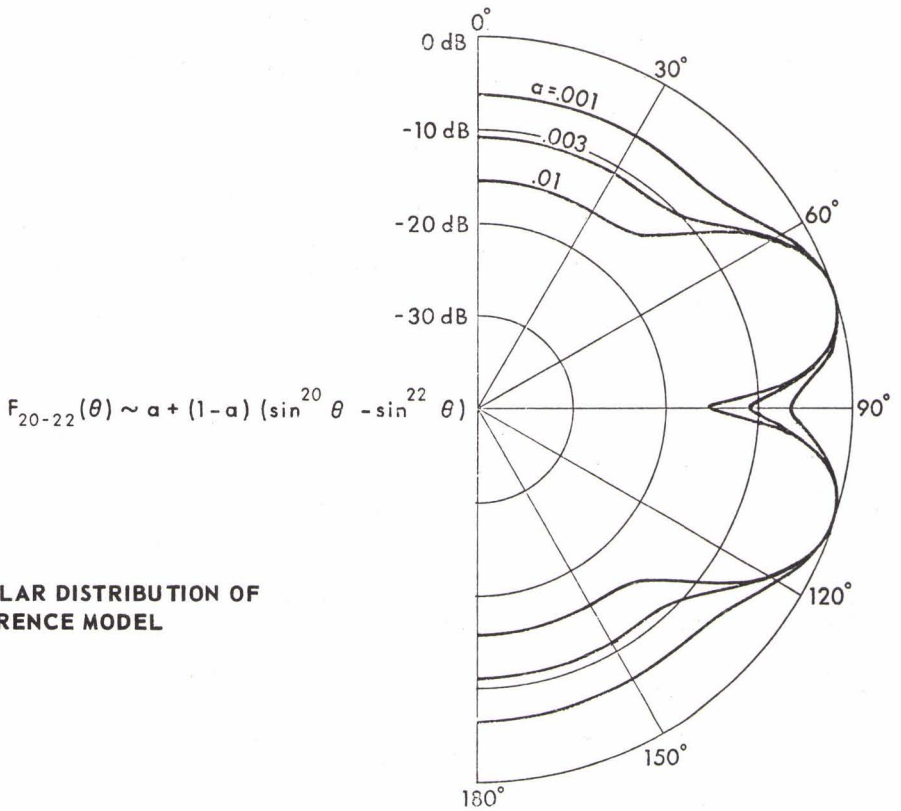

$F_{20-22}(\theta) \sim a + (1-a)(\sin^{20}\theta - \sin^{22}\theta)$

FIG. 6
POLAR PLOTS OF ANGULAR DISTRIBUTION OF POWER FOR THE DIFFERENCE MODEL

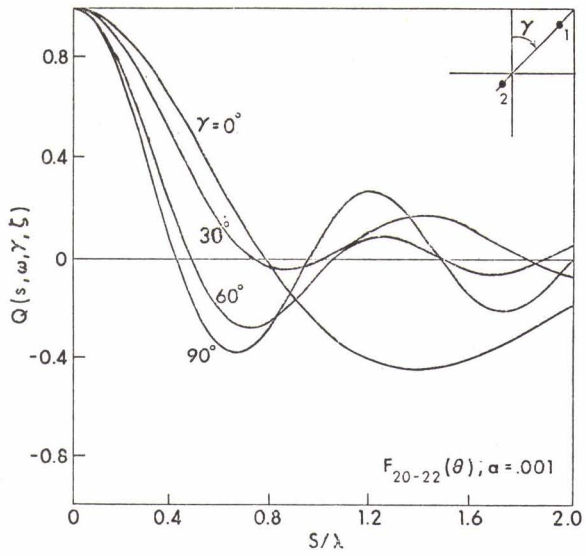

FIG. 7 CROSS-SPECTRAL DENSITY FUNCTIONS FOR VARIOUS SENSOR ORIENTATIONS AND SPACINGS BASED ON THE DIFFERENCE MODEL

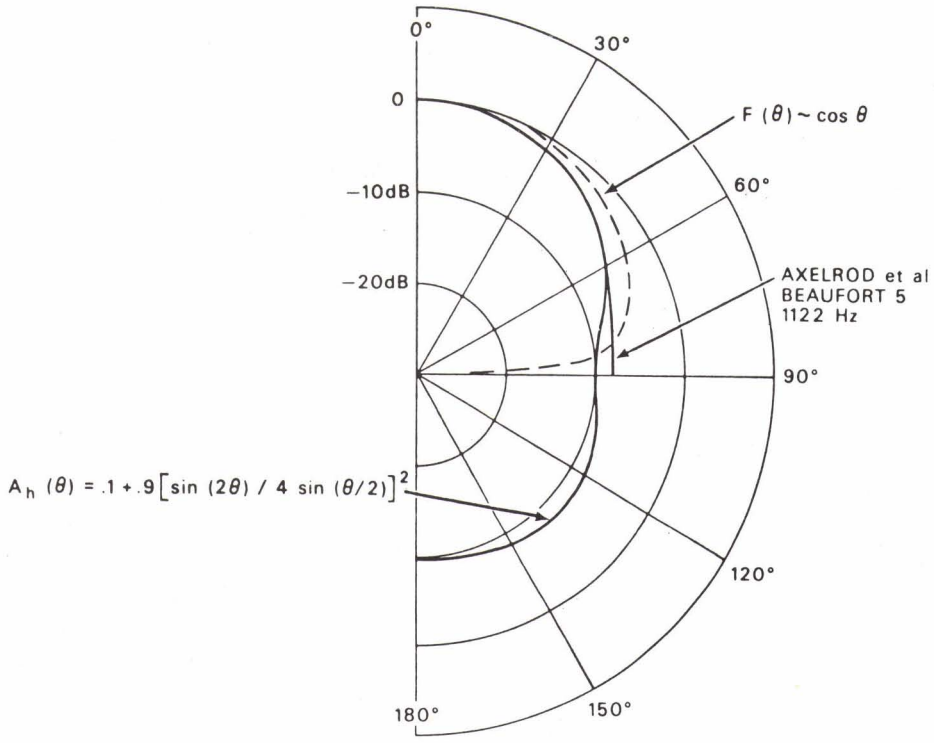

FIG. 8 COMPARISON OF CRON AND SHERMAN MODEL, $A_h(\theta)$ MODEL AND HIGH FREQUENCY MEASUREMENTS OF AXELROD, SCHOOMER AND VON WINKLE (From Ref. 3)

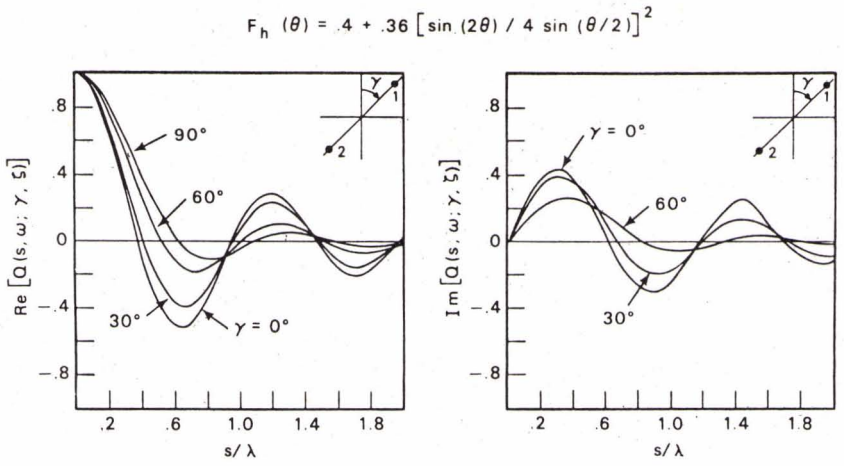

FIG. 9 REAL AND IMAGINARY PARTS OF CROSS-SPECTRAL DENSITY FUNCTIONS FOR VARIOUS SENSOR ORIENTATIONS AND SPACINGS BASED ON $F_h(\theta)$ MODEL (From Ref. 3)

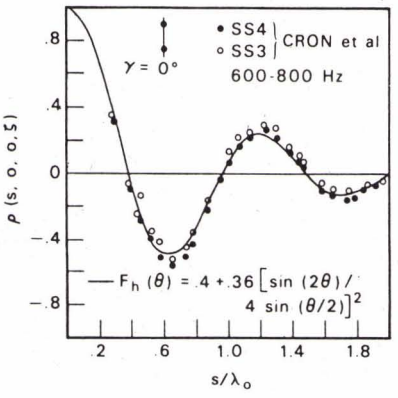

FIG. 10
COMPARISON OF NORMALIZED ZERO TIME-DELAY SPATIAL CORRELATION MEASUREMENTS OF CRON, HASSELL AND KELTONIC WITH THAT DERIVED FROM THE $F_h(\theta)$ MODEL IN THE 600-800 HERTZ BAND (From Ref. 3)

FIG. 11
COMPARISON OF NORMALIZED ZERO TIME-DELAY SPATIAL CORRELATION MEASUREMENTS OF CRON, HASSELL AND KELTONIC WITH THAT DERIVED FROM THE $F_h(\theta)$ MODEL MODEL IN THE 400-600 HERTZ BAND (From Ref. 3)

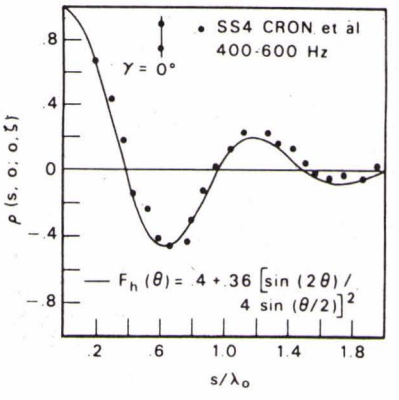

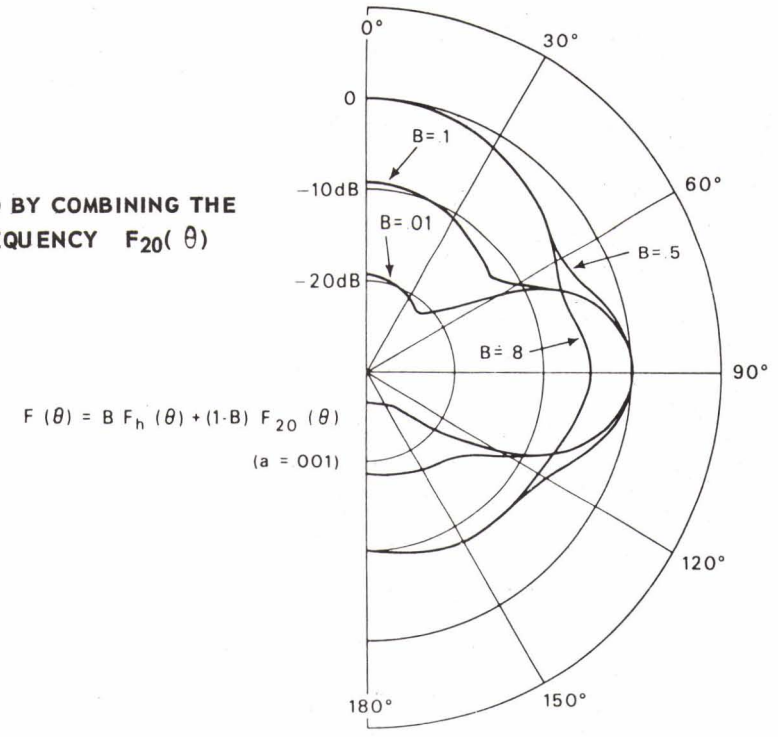

FIG. 12
DIRECTIONAL DENSITY FUNCTIONS OBTAINED BY COMBINING THE HIGH FREQUENCY $F_h(\theta)$ AND THE LOW FREQUENCY $F_{20}(\theta)$ MODELS (From Ref. 3)

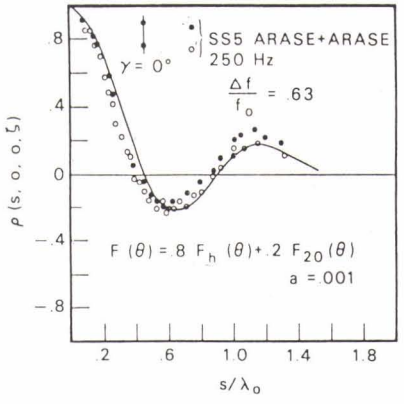

FIG. 13
COMPARISON OF NORMALIZED ZERO TIME-DELAY SPATIAL CORRELATION MEASUREMENTS OF ARASE AND ARASE AT 250 HERTZ WITH THAT DERIVED USING A MIXTURE OF THE $F_h(\theta)$ AND $F_{20}(\theta)$ MODELS WITH 80% OF THE NOISE POWER ATTRIBUTED TO $F_h(\theta)$ (From Ref. 3)

TABLE I. Coefficients for expansion of $\sin^{2m}\theta$ in Legendre polynomials for m = 4 and m = 10. **(From Ref. 3)**

	m = 4	m = 10
a_0	0.40635	0.27026
a_2	-0.73882	-0.58752
a_4	0.46034	0.57107
a_6	-0.14776	-0.40735
a_8	1.98912×10^{-2}	0.22501
a_{10}	0	-9.68372×10^{-2}
a_{12}	0	3.20229×10^{-2}
a_{14}	0	-7.88417×10^{-3}
a_{16}	0	1.36393×10^{-3}
a_{18}	0	-1.48133×10^{-4}
a_{20}	0	7.60684×10^{-5}